Published in IET Signal Processing
Received on 2nd May 2014
Revised on 7th August 2014
Accepted on 12th August 2014
doi: 10.1049/iet-spr.2014.0186

ISSN 1751-9675

Processing algorithms for three-dimensional data compression of ultrasonic radio frequency signals

Pramod Govindan, Jafar Saniie

Department of Electrical and Computer Engineering, Illinois Institute of Technology, Chicago, Illinois 60616, USA
E-mail: saniie@iit.edu

Abstract: Ultrasonic systems are widely used in imaging applications for non-destructive evaluation, quality assurance and medical diagnosis. These applications require large volumes of data to be processed, stored and/or transmitted in real-time. Therefore it is essential to compress the acquired ultrasonic radio frequency (RF) signal without inadvertently degrading desirable signal features. In this paper, two algorithms for ultrasonic signal compression are analysed based on: sub-band elimination using discrete wavelet transform; and decimation/interpolation using time-shift property of Fourier transform. Both algorithms offer high signal reconstruction quality with a peak signal-to-noise ratio (PSNR) between 36 to 39 dB for minimum 80% compression. The computational loads and signal reconstruction quality are examined in order to determine the best compression method in terms of the choice of DWT kernel, sub-band decomposition architecture and computational efficiency. Furthermore, for compressing a large amount of volumetric information, three-dimensional (3D) compression algorithms are designed by utilising the temporal and spatial correlation properties of the ultrasonic RF signals. The performance analysis indicates that the 3D compression algorithm presented in this paper offers an overall 3D compression ratio of 95% with a minimum PSNR of 27 dB.

1 Introduction

One of the major challenges in ultrasonic imaging applications is the large volumes of radio frequency (RF) data. Therefore ultrasonic RF signal has to be compressed as much as possible without degrading the reconstruction quality. The compressed data can be rapidly transmitted to remote locations for archiving and further analysis. Raw RF signal preserves the important information within the signal [1] with direct and precise interpretation for medical diagnosis. In ultrasonic non-destructive evaluation applications, the backscattered RF signal has information about the geometric shape, size and orientation of the scatterers within the propagation path [2, 3].

By analysing the requirements of the ultrasonic imaging applications, it can be agreed that finer details within the signal are highly critical for tissue characterisation, detection and estimation of defects within materials. Therefore compressed ultrasonic RF signal has to be strictly recoverable with very high signal accuracy. For high-definition data and detecting small and transient features within the signal, it is a general practice to sample the signals at much higher rate than one analytically may require (Nyquist rate) capturing the essence of the signal. This oversampling helps to obtain a high time resolution so that the arrival time and the amplitude of the echoes can be precisely detected. However, oversampling generates huge amount of data with redundant information, which has to be removed during compression. Hence, we analyse two methods for ultrasonic RF signal compression with the objective to maintain high compression ratio and high signal reconstruction quality. These methods are: (i) Discrete wavelet transform (DWT) [4, 5] based compression using sub-band elimination, and reconstruction using inverse DWT (IDWT); and (ii) Compression using decimation, and reconstruction using interpolation by utilising the shift properties of Fourier transform.

The uniqueness of DWT is that the multistage sub-band decomposition structure can be carefully designed to isolate the high energy sub-bands. Furthermore, by choosing the most suitable wavelet kernel, different types of signals can be efficiently compressed based on the frequency localisation. In this study, the compression performance is analysed on both the broadband and narrowband echoes for various wavelet kernels. These results are extremely important because of the changes in behavior of the compression algorithms with changes in bandwidth and selection of wavelet kernel. On the other hand, compression by decimation does not involve any computations. The shift-property of Fourier transform is used to recover the decimated samples and to interpolate and reconstruct the signal, including the actual peaks of the signal which might have missed because of decimation.

The performance of the compression is analysed based on the following parameters: peak-signal-to-noise-ratio (PSNR), compression ratio (CR) and correlation coefficients between the original signal and the reconstructed signal. PSNR is defined as $20 \log_{10}(\rho/\sigma)$, where ρ is the maximum sample value in original A-scan and σ is the root mean square error between the original and the reconstructed signal samples.

PSNR is a practical indicator of the overall quality of signal reconstruction. The algorithms discussed in this study emphasise on achieving high PSNR with maximum CR. Furthermore, the similarities between original and reconstructed signal features such as peaks are directly examined and supported by signal correlation characteristics.

Volumetric information demands three-dimensional (3D) scanning and consequently considerable RF signal data collection. Therefore the compression of volumetric RF data becomes an essential part of the data analysis and diagnostic process. In this study, the compression is performed on 3D block of data through successive 1D compression on each of the three directions (x, y and z). In particular, we analyse how the PSNR varies depending on the CR and the correlation properties among 3D ultrasonic experimental measurements.

This paper is organised as follows. Section 2 examines the application of DWT for compressing ultrasonic RF signals with the emphasis on achieving maximum compaction for narrowband and broadband ultrasonic echoes. Section 3 provides an alternate method for compressing ultrasonic RF signal by decimation. This section also presents a detailed mathematical analysis for interpolation and recovery of the compressed RF signals. Section 4 evaluates the signal reconstruction quality and computational loads of DWT and decimation based compression methods. Section 5 presents the design and analysis of 3D data compression techniques applied to ultrasonic experimental data.

2 DWT based compression

Certain signal transforms are suitable for data compression because of their data decorrelation and energy compaction properties. For example, discrete transforms such as Karhunen–Loeve transform (KLT), discrete cosine transform (DCT) [6], Walsh–Hadamard transform (WHT) [7] and DWT [4] have these properties to various extents. Even though KLT gives optimal data compression, the data dependence of the KLT kernel limits its application for practical purposes. On the other hand, DCT, WHT and DWT are data independent and thus facilitate efficient implementations of the compression algorithms [8, 9]. The data compression performance varies based on the ultrasonic echo shape and signal bandwidth. DWT is superior in the compression of broadband ultrasonic RF signals, while DCT and WHT perform better for the compression of narrowband signals [9].

Multilevel DWT performs sub-band decomposition using lowpass and highpass filters, wherein a significant portion of the signal energy is localised in the low frequency region for ultrasonic applications [5]. This approach is known as wavelet packet decomposition and it is shown in Fig. 1 for a 4-level sub-band decomposition. The sub-bands with very low energy can be eliminated [10]. Since location and size of the eliminated sub-bands within the whole spectrum are pre-determined, signal information for these sub-bands are not stored and/or transmitted. The higher the sampling frequency compared with the Nyquist rate, the more levels of decomposition is possible, which allows better isolation of high energy sub-bands to maximise compaction with high signal reconstruction quality.

To demonstrate the efficiency of wavelet packet decomposition, an ultrasonic A-scan with 2048 samples consisting of many reflected and interfering echoes as shown in Fig. 2*a* is decomposed using DWT structure shown in Fig. 1. Fig. 2*b* shows the decomposed sub-bands {LLLL, LLLHL, LLLHH, LLHL, LLHH, LH, H}, which indicates that the actual information within the signal is localised into the low frequency sub-bands.

Fig. 2*b* confirms that H, LH and LLHL sub-bands which constitute 79% of the signal samples have almost zero energy and can be discarded, indicating 79% compression.

Ultrasonic RF signals in general fall into two categories based on their bandwidth, referred to as broadband and narrowband. Broadband transducer may need to be utilised in order to acquire high resolution signal for detecting and isolating multiple echoes corresponding to physical characteristics of complex objects. However, narrowband transducer is suitable for higher detection sensitivity [11] and imaging deep within the objects. The performance of DWT based compression for broadband and narrowband differs depending on the wavelet kernels used for compressing the signals. Therefore in this study, both broadband and narrowband signals are analysed for their compression performance.

The best compaction can be achieved by properly choosing the right wavelet kernel to decompose the ultrasonic signal. The kernel must be chosen for best compaction such that energies of most of the sub-bands are small, and can be eliminated without affecting quality of signal reconstruction. This scenario depends on regularity, number of vanishing moments of scaling function of the kernel and size of the support [12, 13]. Compactly supported wavelets are most suitable to analyse high frequency components [13]. Therefore four orthogonal and compactly supported wavelets namely Haar [14], Daubechis [13], Symmlets and Coiflets [14] are used in decomposing ultrasonic RF signals to analyse the experimental results to decide the right wavelet kernel offering maximum compaction. Daubechies (Db) wavelets are orthogonal, compactly supported and

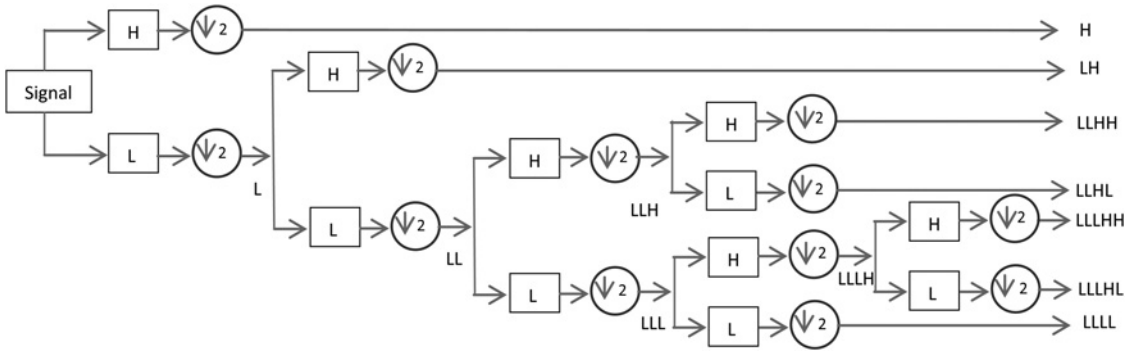

Fig. 1 *DWT 4-level wavelet packet decomposition*

IET Signal Process., 2015, Vol. 9, Iss. 3, pp. 267–276
doi: 10.1049/iet-spr.2014.0186

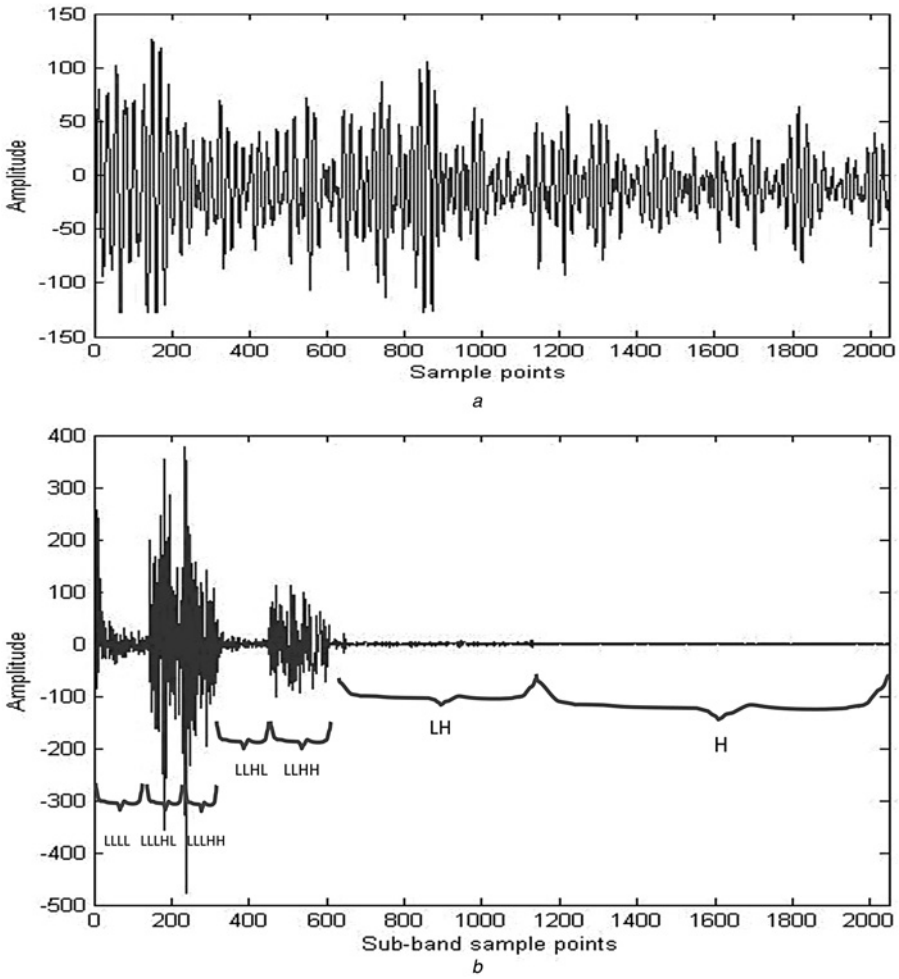

Fig. 2 *Ultrasonic A-scan with 2048 samples consisting of many reflected and interfering echoes and the decomposed sub-bands*

a Ultrasonic A-scan with 2048 samples with the sampling rate of 100 MHz using 5 MHz ultrasonic transducer
b Four-level DWT coefficient plot within sub-bands of the A-scan

continuous. The high similarity between the Daubechies10 (Db10) wavelet function [13] and ultrasonic echo [15] indicates that Db10 will be more suitable for compacting ultrasonic echoes. This is confirmed by our experimental results given in Table 1. By increasing the support width, Db wavelet becomes smoother and provides better frequency localisation.

In pulse-echo ultrasonic testing, the backscattered echo from a flat surface reflector or point reflector can be modelled as Gaussian echo [15], $s(\theta; t) = \beta e^{-\alpha(t-\tau)^2} \cos\left(2\pi f_c(t-\tau)+\phi\right)$ where the signal parameters of the echo are α, the bandwidth factor, τ, the arrival time, f_c, the centre frequency, ϕ, the phase and β, the amplitude. Gaussian function is suitable for time-frequency analysis because it is optimally concentrated in both time and frequency. For a Gaussian echo, bandwidth that contains 98% of the signal energy is $\mathrm{BW}_{98\%} = 0.382\sqrt{\alpha}$ [15]. The normalised BW (which is the inverse of Q-factor) is expressed as $\eta_{\mathrm{BW}} = 0.382\sqrt{\alpha}/f_c$, where f_c is the centre frequency. For this study, $\eta_{\mathrm{BW}} = 0.5$ is considered as narrowband. η_{BW} value >0.5 is considered broadband. To analyse the performance of wavelet kernels for broadband and narrowband signals, Gaussian echoes with η_{BW} ranging from 0.2 to 0.8 are generated and sampled at 100 MHz. A 3-level DWT is performed on these echo samples. 15 most dominant DWT coefficients are preserved, and the remaining coefficients are eliminated. This provides 93% compression.

Table 1 PSNR and correlation coefficient results for compression of broadband and narrowband Gaussian echo using various wavelet kernels

	Broadband echo ($\eta_{\mathrm{BW}} = 0.8$)		Narrowband echo ($\eta_{\mathrm{BW}} = 0.5$)	
	PSNR, dB	Correlation coefficient	PSNR, dB	Correlation coefficient
Db10	44.15	0.9995	34.52	0.9970
Haar	29.26	0.9840	23.57	0.9625
Coif1	34.48	0.9952	28.23	0.9873
Sym2	36.12	0.9967	28.64	0.9885

The PSNR and correlation coefficient between original and reconstructed echoes are calculated for both broadband and narrowband echoes as shown in Table 1. This table shows that DWT performs superior for broadband signals compared with narrowband signals, and Db10 is the best kernel for signal compaction.

Energy of the 15 preserved coefficients for the various wavelet kernels is analysed over a wide range of frequency bands to differentiate the performance of these wavelet kernels in broadband and narrowband regions. Energy compaction values (Ratio between Energy with only 15

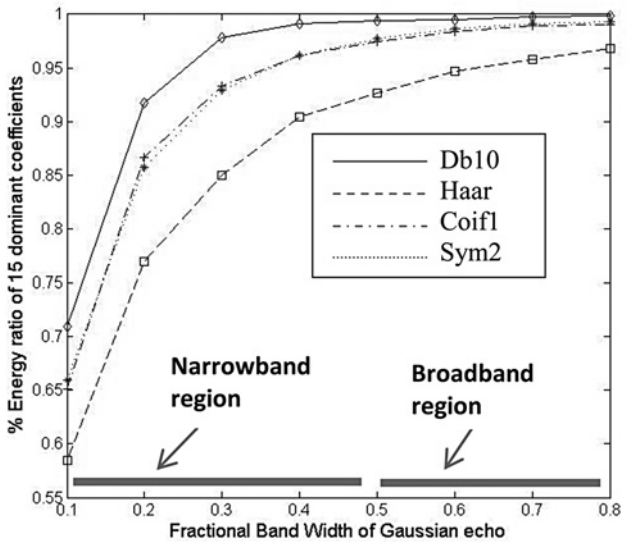

Fig. 3 *Energy compaction values of 15 most dominant coefficients for narrowband and broadband echoes*

dominant coefficients and Energy with all coefficients) for narrowband and broadband echoes are plotted in Fig. 3. From the plot, it is clear that all wavelet kernels perform well (allows maximum compression) in the broadband region, however Db10 performs better including the narrowband region.

3 Decimation and time-shift interpolation

The ultrasonic RF signal is usually oversampled to avoid aliasing effect and also to provide high resolution sampled information for detecting the precise amplitude and arrival time of the echoes. In practice, the signal may contain unwanted frequency components such as noise with a much higher frequency band compared with Nyquist frequency of the most wanted RF signal. Consequently, oversampling decreases the impact of the fold-over frequency (i.e. aliasing) and the unwanted high frequency components will not be aliased into the desirable band of the signal. Oversampling creates redundant signal information that can be removed by performing signal decimation without violating the Nyquist sampling rate. However, to improve the time resolution of decimated signal as may be required in certain applications, we developed and analysed an efficient interpolation method which utilises time-shift properties of Fourier transform as explained in the following sections.

The most common interpolation process is linear interpolation. This method results in acceptable error by choosing a sampling rate several times higher than the rate required by the sampling theorem. To remove the inadequecies, higher order polynomials have to be used for interpolation. Here, a practical interpolation technique is developed which incorporates time-shift property of Fourier transform. This method is highly efficient for reconstruction of decimated/compressed ultrasonic signal.

Consider a signal $s(t)$ sampled with a sample interval T and N number of samples

$$\hat{s}(t) = \sum_{k=0}^{N-1} s(kT)\delta(t - kT) \tag{1}$$

The values of $\hat{s}\ (t)$ are only known at kT where $k = 0, 1, 2,\ldots, N–1$

$$\left[s(nT)\right] = s(0), s(T), s(2T), \ \ldots..s\big((N-1)T\big) \tag{2}$$

The discrete Fourier transform of the above sequence is defined as

$$S(k\Omega) = \sum_{k=0}^{N-1} s(nT)\mathrm{e}^{-\mathrm{j}k\Omega nT} \tag{3a}$$

where

$$\Omega = \frac{2\pi}{NT} \tag{3b}$$

With this definition, $S(\mathrm{k}\Omega)$ has N distinct values and is periodic with period $\mathrm{N}\Omega$

$$S(k\Omega) = S(k\Omega + rN\Omega);\ r = 0,\ \pm1,\ \pm2,\ \ldots \tag{3c}$$

The original time sequence can be recovered uniquely from (3a)

$$s(nT) = F^{-1}(S(k\Omega)) = \frac{1}{N}\sum_{k=0}^{N-1} S(k\Omega)\mathrm{e}^{\mathrm{j}k\Omega nT} \tag{4}$$

The discrete inverse Fourier transform exhibits periodicity in the same manner as the discrete Fourier transform. Hence

$$s(nT) = s(nT + rNT);\ r = 0,\ \pm1,\ \pm2,\ \ldots. \tag{5}$$

The function $s(t)$ for a given number of samples can be approximated as [16, 17]

$$s(t) \cong \mathrm{T}\sum_{n=0}^{N-1} s(nT)\frac{\sin(2\pi/T)(t-nT)}{\pi(t-nT)} \tag{6}$$

where

$$0 \le t \le (N-1)T \tag{7}$$

Any value of the function between the samples can be estimated directly from the above interpolation equation. Major drawback of this type of interpolation is the lack of computational efficiencies. An alternate interpolation method would be to use time-shift property of discrete Fourier transform. If $s(nT)$ is shifted by $\Delta t < \mathrm{T}$, then

$$s(nT - \Delta t) <=> S(k\Omega)\mathrm{e}^{-\mathrm{j}k\Omega\Delta t} \tag{8}$$

To verify the above equation, we substitute $nT - \Delta t$ for parameter nT in (4)

$$s(nT - \Delta t) = \frac{1}{N}\sum_{k=0}^{N-1}\left[S(k\Omega)\mathrm{e}^{-\mathrm{j}k\Omega\Delta T}\right]\mathrm{e}^{\mathrm{j}k\Omega nT} \tag{9}$$

By direct inspection of the above equation , it can be seen that the terms in brackets are the discrete Fourier transform of $s(nT–\Delta t)$. Therefore by finding the discrete Fourier transform of the measured sequence and multiplying it by $\mathrm{e}^{-\mathrm{j}k\Omega\Delta T}$, one can determine the discrete Fourier transform of

doi: 10.1049/iet-spr.2014.0186

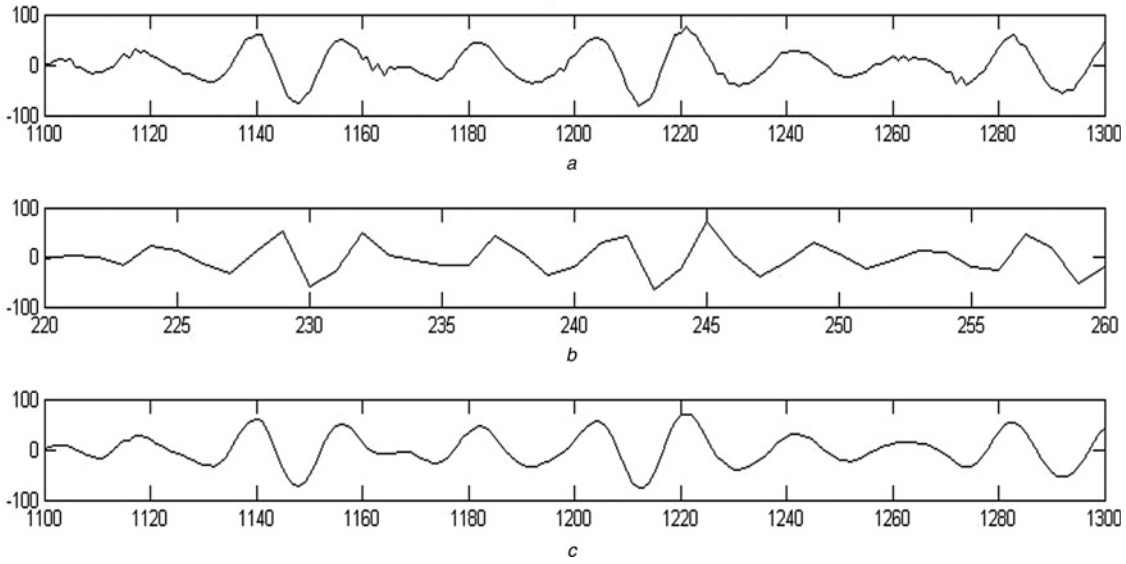

Fig. 4 *Ultrasonic signal decimation for 80% compression and signal reconstruction by time-shift interpolation, applied on the A-scan signal shown in Fig. 2a [Only a portion of the original and reconstructed signals are shown here for better clarity]*

a Original A-scan
b Original A-scan-decimated by 5
c Reconstructed A-scan-after time-shift interpolation

the intermediate points. Finally, the inverse Fourier transform of this term yields the desired interpolated points. The interpolated sequence obtained by the time-shift method contains all the information of the original sequence. The steps for the decimation and time-shift interpolation algorithm applied on the A-scan signal shown in Fig. 2*a* are described below.

(1) Decimate the original signal by a factor M (portion of original A-scan signal and decimated signal with $M = 5$ are shown in Figs. 4*a* and *b*, respectively).
(2) Perform FFT of the decimated signal.
(3) Time-shift the output of Step 2 by multiplying it with $e^{-jk\Omega(mT/M)}$ for $m = 1, 2, 3, ..., M-1$
where, k is an integer which varies from 1 to N (N is the number of samples in the time-shifted signal).
(4) Get the Hermitian conjugate of the spectrums obtained from Step 3, reverse the elements and append it to the spectrum of Step 3 to form the complete spectrum.
(5) Perform IFFT of the spectrums obtained from Step 4.
(6) Interleave the time domain signals obtained from Step 5 with the decimated signal from Step 1. This retrieves the original signal.(portion of retrieved signal is shown in Fig. 4*c*).

Decimation by 5 (Fig. 4*b*) provides 80% compression and does not require any computations. The signal reconstructed by using time-shift interpolation (see Fig. 4*c*) follows the original signal with high accuracy. The difference between Figs. 4*a* and *c* is only because of the high frequency measurement noise existing in Fig. 4*a*, which was removed by the process of interpolation as shown in Fig. 4*c*.

The peaks which might have lost during the process of decimation can be very precisely retrieved by calculating a Δt shift which is the time-shift of the peak of decimated signal from the peak of the original signal. The interesting feature of this method is that it not only identifies the actual peak value, but also finds the exact time instance at which the peak occurs. In the measured ultrasonic signal, the time corresponding to the position of the absolute value of the largest peak is considered to be the reference point, t_{ref}. The largest peak is chosen because of its high signal-to-noise ratio. Furthermore, the Δt computation is performed only for the largest peak. The t_{ref} must be one of the sample points, but this is not normally the case because of signal decimation for compression.

The t_{ref} of an analytic function $s(t)$ can be obtained by

$$\frac{\partial s(t)}{\partial t} = 0 \tag{10}$$

Let us approximate the time limited $s(t)$ in terms of a set of orthogonal exponential functions (Fourier series expansion)

$$s(t) = \sum_{k=(-N/2)}^{N/2} S(k\Omega)e^{jk\Omega t};\ 0 \le t \le NT \tag{11a}$$

where $S(k\Omega)$ are Fourier series coefficients, and

$$\Omega = \frac{2\pi}{NT} \tag{11b}$$

Substituting (11a) into (10) will yield

$$\sum_{k=(-N/2)}^{(N/2)} kS(k\Omega)e^{jk\Omega t} = 0 \tag{12}$$

In the above non-linear equation, an explicit solution for t is not possible. However, one can make the assumption that t_{ref} is located near a given time t_0 by an unknown time Δt

$$t = t_0 + \Delta t \tag{13}$$

Rewriting (12) in terms of $t_0 + \Delta t$

$$\sum_{k=(-N/2)}^{N/2} kS(k\Omega)e^{jk\Omega t_0}e^{jk\Omega \Delta t} = 0 \tag{14}$$

Let

$$R_k = \text{Real } S(k\Omega)e^{jk\Omega t_0}; \quad I_k = \text{Imag } S(k\Omega)e^{jk\Omega t_0} \tag{15}$$

Then, (14) becomes

$$\sum_{k=(-N/2)}^{N/2} k\left[R_k \cos(k\Omega\Delta t) - I_k \sin(k\Omega\Delta t)\right] = 0 \tag{16a}$$

$$\sum_{k=(-N/2)}^{N/2} k\left[I_k \cos(k\Omega\Delta t) + R_k \sin(k\Omega\Delta t)\right] = 0 \tag{16b}$$

For sufficiently small Δt, the Taylor series expansion of sine and cosine can be approximated

$$\sin(k\Omega\Delta t) \simeq k\Omega\Delta t; \ \cos(k\Omega\Delta t) \simeq 1 - \frac{(k\Omega\Delta t)^2}{2} \tag{17}$$

With such an approximation, (16a) and (16b) becomes

$$\left[\sum_{k=(-N/2)}^{(N/2)} kR_k\right] - \frac{1}{2}\left[\sum_{k=-N/2}^{N/2} k^3 R_k\right]\Omega^2\Delta t^2 - \left[\sum_{k=-N/2}^{N/2} k^2 I_k\right]\Omega\Delta t = 0 \tag{18a}$$

$$\left[\sum_{k=-N/2}^{N/2} kI_k\right] - \frac{1}{2}\left[\sum_{k=-N/2}^{N/2} k^3 I_k\right]\Omega^2\Delta t^2 + \left[\sum_{k=-N/2}^{N/2} k^2 R_k\right]\Omega\Delta t = 0 \tag{18b}$$

In (18a), all terms in brackets are zero since they are samples of odd functions and are summed from $-N/2$ to $+N/2$. Solutions of the quadratic (18b) in Δt can be obtained as

$$\Delta t = \frac{1}{\Omega}\frac{-b \pm \sqrt{b^2 + 4ac}}{-2a} \tag{19}$$

where

$$a = -\frac{1}{2}\sum_{k=-N/2}^{N/2} k^3 I_k; \quad b = \sum_{k=-N/2}^{N/2} k^2 R_k; \quad c = \sum_{k=-N/2}^{N/2} kI_k \tag{20}$$

From the two possible solutions of Δt given in (19), we choose one that gives the maximum absolute value of $s(t)$. Equation (18b) has been derived from an approximation for which Δt does not in general yield the optimal solution. Therefore an iterative method is adopted which can be shown as

$$t_i = t_{i-1} + \Delta t_i; \quad i = 1, 2, \ldots, \text{etc} \tag{21}$$

where Δt_i is an estimated time shift in ith iteration. Practically, the search for optimal solution is terminated when the condition

$$|\Delta t_i| \leq 10^{-4} T \tag{22}$$

is satisfied. In the above inequality, T is the sampling interval of the decimated signal.

The following steps explain the Δt computation.

(1) Locate the time, $t_0 = kT$, (k is an integer) which is expected to be the closest to t_{ref} and corresponds to the location of the data sequence such that

$$s(t_0) = \text{Max}\left[|s(nT)|; n = 0, 1, 2, \ldots, N\right] \tag{23}$$

(2) Estimate the Fourier transform of the signal.
(3) Use the discrete Fourier transform values for solving (19).
(4) Compute the shifted time sequence by (9); and check for the feasibility of the present shift by the following:

$$|s(t_{i+1})| > |s(t_i)| \tag{24}$$

(5) If terminating criterion (see (22)) is satisfied, go to the next step, otherwise replace t_i by t_{i+1} and go to Step 2.
(6) Optimal reference time is determined, $t_{\text{ref}} = t_i$; preserve the shifted data for further signal processing.

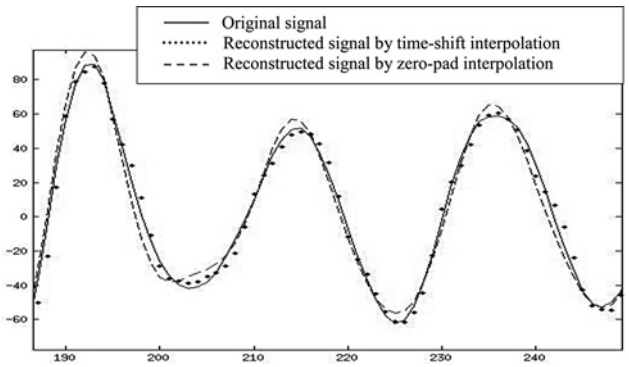

Fig. 5 *Reconstructed signals by time-shift and zero-pad interpolation techniques*

From Fig. 5, we can see that reconstruction by time-shift interpolation follows the original signal very well, especially the peaks. Solid line represents the original signal. Dotted line, which is the reconstructed signal by time-shift interpolation, exactly follows the original signal, whereas the dashed line, which represents the reconstructed signal using frequency domain zero-pad expansion of the decimated signal (i.e. a simple and efficient signal interpolation method), does not exactly follow the original signal, especially the desirable peaks.

4 Reconstruction quality and computational loads

RF signal reconstruction quality and computational loads vary according to the type of compression and reconstruction methods. In this study, two methods are examined: Compression by DWT and reconstruction by IDWT (referred to as method-1); and Compression by

doi: 10.1049/iet-spr.2014.0186

Table 2 Performance of compression schemes applied to ultrasonic A-scans

Compression method	Reconstruction method	PSNR, dB	Correlation coefficient	Reconstruction quality	Computational speed	Resource utilisation
DWT	IDWT	35.63	0.9984	high	low	low
decimation	time-shift interpolation	38.68	0.9949	high	high	high

Ultrasonic A-scan shown in Fig. 2*a* is used for both methods. Db10 wavelet is used for DWT/ IDWT, and $d = 5$ is chosen for decimation

decimation and reconstruction by time-shift interpolation (referred to as method-2).

By carefully selecting the proper decimation factor according to the sampling rate, the decimation procedure ensures that none of the actual RF signal information, including the transient and finer details, is removed during compression (decimation). In time-shift interpolation of the decimated signals, all discarded samples are accurately retrieved and thus the PSNR becomes high. This is also true for DWT and IDWT because of the perfect reconstruction characteristics of the quadrature mirror filters used in decomposition and reconstruction phase.

In this study, computational speed for the compression schemes are analysed by calculating total number of cycles required to perform various operations during compression and reconstruction. Multiplication is the major operation affecting computational performance of the compression algorithms. We assume one 16-bit × 16-bit multiplication executes in one clock cycle. Let N be the number of samples in the original signal and d be the decimation factor. One N-point FFT execution requires $2N\log2(N)$ multiplications [18]. Operations that need computations are only considered for this performance analysis. (Operations such as elimination of samples or re-organisation of samples are assumed to consume very little time compared with complex operations such as FFT and multiplications).

DWT/IDWT requires filtering and sub-sampling/ up-sampling operations. DWT with 4-level decomposition is considered for computational performance analysis. The lowpass and highpass filters are processed in parallel, and filtering operation requires 10 cycles for Db10 wavelet [19]. First level of decomposition requires filtering of N samples. The following levels contain only half the samples from previous levels. Therefore the second level needs filtering of $N/2$ samples. The third level requires filtering of $N/4$ samples and the fourth level requires filtering of $N/8$ samples. IDWT requires exactly the same number of operations, but in the reverse order. Therefore overall computation time τ_1 for method-1 (Compression by DWT and reconstruction by IDWT) is

$$\tau_1 = 2(10)\left(N + \frac{N}{2} + \frac{N}{4} + \frac{N}{8}\right) = \frac{75}{2}N \tag{25}$$

For method-2 (Compression by decimation and reconstruction by time-shift interpolation), the compression does not require any computations. Time-shift interpolation requires one FFT on N/d samples (d is the decimation factor), followed by $(d-1)$ complex multiplications of size N/d, and $(d-1)$ IFFTs on N/d samples. Assuming each complex multiplication needs four multiplication operations, total computation time τ_2 for method-2 is

$$\tau_2 = 2d\frac{N}{d}\log_2\left(\frac{N}{d}\right) + 4(d-1)\frac{N}{d} \tag{26}$$

For this method, $(d-1)$ multiplications and $(d-1)$ IFFTs can be performed in parallel, at the expense of additional hardware resources. Consequently the computational time will be reduced to

$$\tau_{2-\text{fast}} = 4\frac{N}{d}\log_2\left(\frac{N}{d}\right) + 4\frac{N}{d} \tag{27}$$

The performance for both methods is summarised in Table 2, which indicates that both methods offer high signal reconstruction quality. Method-1 requires only one lowpass and one highpass filter, and is most suitable for an application where low resource utilisation is desirable. Method-2 with parallel operations is recommended for an application which requires high computational speed at the expense of large number of hardware resources because of FFT and multiple IFFT modules.

5 Ultrasonic data acquisition and 3D data compression

Medical imaging as well as industrial NDE applications requires processing of volumetric information. This information is collected by the process of 3D scanning and massive RF signal data acquisition. Therefore careful analysis is required to acquire and compress 3D volumetric RF data. For this study, the performance of 3D compression is evaluated using both DWT and decimation/interpolation methods.

In volumetric ultrasonic data compression, data sets (slices) are organised into a 3D block (128*128*2048 samples) as shown in Fig. 6*a* and consequently this block of data is compressed to remove the inter-slice data redundancy in x, y and z directions as shown in Fig. 6*b*.

The experimental data was generated using a steel block specimen and a 5 MHz, 0.375″ diameter ultrasonic transducer. A 2″ × 2″ surface of the steel block was scanned for inspection. The step size (distance between each measurement point) is kept as 0.44 mm to ensure no information is missed within the specimen.

High frequency ultrasonic RF signal introduces high spatial resolution during the data acquisition process. Although the neighbouring A-scans are highly correlated, they may be misaligned by a few samples. Cross correlation between two neighbouring A-scans can be used to find a good estimate of misalignment between two neighbouring measurements. The cross correlation estimate for A-scan 'p' and A-scan 'q' can be expressed as (see (28) at the bottom of the next page)

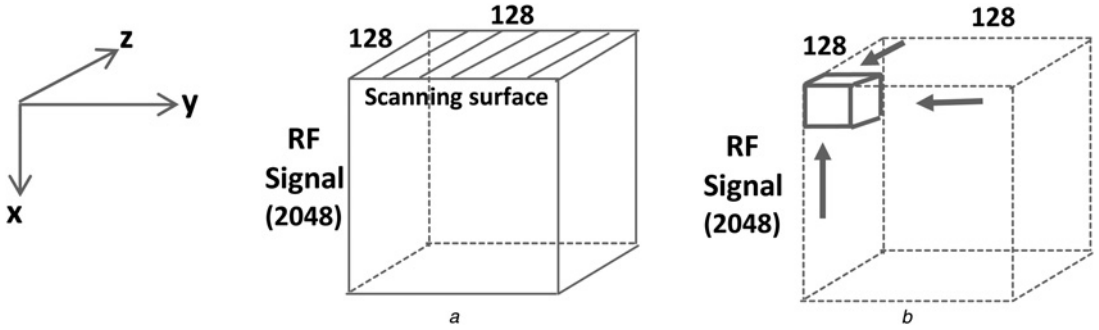

Fig. 6 *Data sets (slices) are organised into a 3D block*

a 3D ultrasonic data block
b 3D compressed data

We can choose one particular A-scan in a row (as the reference A-scan), and calculate the relative shift, m, of all other A-scans with respect to the reference A-scan. The optimal relative shift of A-scan 'p' with respect to A-scan 'q', $m_{p,q}$, can be expressed as

$$m_{p,q} = \max_{m}\left\{R_{p,q}[m]\right\} \tag{29}$$

Since the neighbouring A-scans are highly correlated, in practice, the required shifts of the data for signal alignment are only a few samples. If we align the signals to estimate maximum correlation between neighbouring signals, PSNR of the reconstructed signal after compression can be improved.

A study of the correlation coefficients between nearby A-scans is useful in determining the efficiency of compression operation. To analyse the correlation properties between A-scans, eight consecutive A-scans are examined. The Pearson correlation coefficient between the first A-scan and all other seven A-scans are calculated. A correlation coefficient of '1' indicates perfect match between the A-scans. By analysing the correlation coefficients between neighbouring A-scans in the spatial (y and z) directions, it became clear that nearby A-scans are highly correlated, which allows a high degree of compression without sacrificing original signal information.

In this study, 3D DWT compression is performed in three successive steps [20]. In the first step, all A-scans in x-direction are compressed by using 1D DWT. This is followed by another 1D DWT in y-direction across the x-z-plane. Finally, 1D DWT is performed in z-direction across the x-y-plane to form the 3D compressed RF data.

Signal characteristics are more predictable for the A-scans, since it is governed by ultrasonic transducer bandwidth. Therefore predictable and optimal compression can be achieved in x-direction. The optimal compression of A-scans can be best determined by choice of the wavelet kernel and sub-band decomposition structure. In this study, we have examined the compression performance of A-scans using four compactly supported wavelets: Db10, Haar, Coif1 and Sym2. The analysis of energy distribution for these wavelet kernels indicates that Db10 provides the best compression without losing much of the signal energy. Therefore Db10 is the choice for compressing A-scans. To isolate more high energy and compact sub-bands, level-4 wavelet packet decomposition structure (see Fig. 1) is designed.

In our ultrasonic experimental study, there are 128 measurement points per line in y and z directions. Characteristics of these lines are not predictable because of the beam field of the transducer, scanning step size, and material properties. Therefore a 2-level DWT using Haar wavelet is performed, since it is simple and efficient. This provides an additional 75% compression in y-direction and a further 75% compression in z-direction.

DWT by nature de-noises the signal. However, the original RF signal may be noisy which will make it difficult to analyse the reconstruction quality. Therefore we filtered out the noise from original A-scans, so that correlation and PSNR of the original and reconstructed signal can be compared in an unbiased way. Furthermore, when the RF signal is generated by scanning process, because of the slight timing variations between various A-scans, there could be some mis-alignment between the A-scans with respect to time. This is resolved by aligning the A-scans to maximise correlation between neighbouring A-scans.

The 3D compression performance is analysed based on CR, PSNR and correlation coefficient between original and reconstructed A-scans. Overall 3D CR can be improved by careful design of sub-band decomposition structure, where very low energy sub-bands will be determined and discarded. Table 3 shows the compression performance parameter values for various combinations of CRs in x, y and z directions for two scenarios: (i) compression is performed on raw RF signals; and (ii) compression is performed after the raw RF signals are de-noised and aligned. By inspecting Table 3, it can be observed from row-3 that by discarding only 'H' sub-band in x-direction, we achieve 52% compression. Similarly, by discarding H and LH sub-bands in y and z directions, further compression of 75% can be obtained in y and z directions

$$R_{p,q}[m] = \begin{cases} \dfrac{1}{N-|m|}\displaystyle\sum_{n=0}^{N-m-1} p(n+m)\,q(n) & \text{for } 0 \le m \le N-1 \\ \dfrac{1}{N-|m|}\displaystyle\sum_{n=0}^{N-|m|-1} p(n)q(n+|m|) & \text{for } -(N-1) \le m \le 0 \end{cases} \tag{28}$$

doi: 10.1049/iet-spr.2014.0186

Table 3 3D DWT compression results

Row	Axial CRs, %			Overall 3D compression ratio, %	Correlation coefficient (mean)		PSNR (mean)		Eliminated sub-bands (Refer to Fig. 1 for clarification)		
	X	Y	Z		Scenario1	Scenario2	Scenario1	Scenario2	X	Y	Z
1	80	75	75	98.75	0.9208	0.9732	20.48	23.75	H, LH, LLHL	H, LH	H, LH
2	72	75	75	98.25	0.9300	0.9744	20.58	23.97	H, LH	H, LH	H, LH
3	52	75	75	97.00	0.9225	0.9747	20.66	24.00	H	H, LH	H, LH
4	80	0	75	95.00	0.9376	0.9796	21.81	25.00	H, LH, LLHL	–	H, LH
5	80	50	50	95.00	0.9584	0.9860	23.19	26.58	H, LH, LLHL	H	H
6	80	0	50	90.00	0.9674	0.9884	24.11	27.46	H, LH, LLHL	–	H
7	80	50	0	90.00	0.9742	0.9896	24.79	28.00	H, LH, LLHL	H	–
8	52	50	50	88.00	0.9588	0.9878	23.27	27.20	H	H	H
9	80	0	0	80.00	0.9931	0.9976	29.78	34.42	H, LH, LLHL	–	–

*Scenario*1*:* The compression is performed on the raw RF signals. *Scenario*2: The compression is performed after the raw RF signals are de-noised and aligned

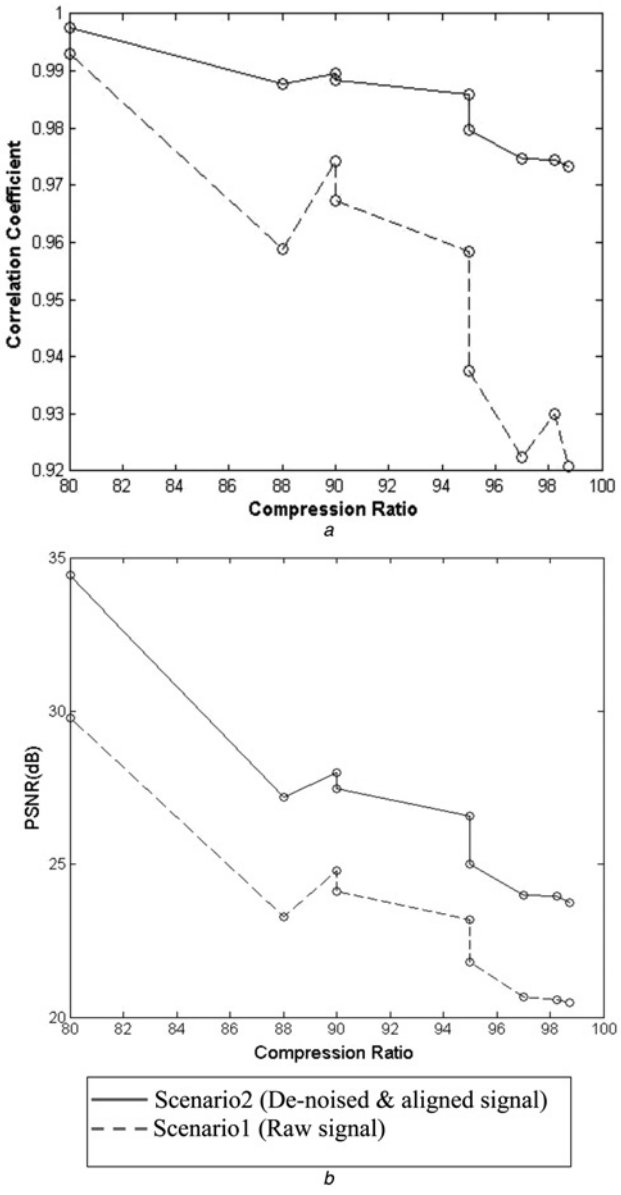

Fig. 7 *Plots of correlation coefficient and PSNR*

a CR against correlation coefficient for two scenarios
b CR against PSNR for two scenarios

individually. Thus, overall 3D CR becomes 97%. Various combinations of axial (x, y or z) CRs can be chosen for higher PSNR and better correlation to improve the signal reconstruction quality. This can be seen from 4th and 5th rows in Table 3 where both provide a 3D CR of 95%. However, the combination given in 5th row (80-50-50) offers better correlation coefficient and PSNR than that in 4th row (80-0-75). Furthermore, the results presented in Table 3 clearly indicate that correlation coefficient and PSNR improves significantly with de-noising and A-scan alignment. As shown in row-1, for a CR of 98.75%, correlation coefficient improved from 0.9208 to 0.9732 and similarly PSNR improved from 20.48 dB to 23.75 dB.

Fig. 7 shows the plots of correlation coefficient [Fig. 7*a*] and PSNR [Fig. 7*b*] with respect to the CR for the values given in Table 3. From these plots, it is clearly apparent that, for improving CR from 80% to 98.75%, correlation coefficient degrades moderately from 0.9976 to 0.9732, and PSNR drops from 34.42 to 23.75 dB. This level of degradation in signal quality because of very high level of compression is tolerable for many practical applications.

The level of compression depends on the step size, degree of oversampling in time and space and transducer beam field. As an alternative to DWT based 3D compression, we have also explored that decimation by 5 in x-direction for compressing A-scans, and decimation by 4 in y and z directions are acceptable for maintaining high signal reconstruction quality. By using decimation method, we obtained a PSNR of 22 dB for an overall CR of 98.75%. Time-shift interpolation method is used for achieving high temporal and spatial resolution using optimally scanned and sampled signal.

6 Conclusion

Ultrasonic imaging applications require processing of large volumes of RF data in real-time. Raw RF data preserves the transient and small features which are significant in many practical applications. Compressing the RF data is essential to accelerate the processing performance and also to transfer the data rapidly to remote locations for expert analysis. Two methods for ultrasonic data compression using DWT based sub-band elimination and decimation/interpolation are analysed with emphasising the quality of signal reconstruction and computational speeds. In particular, this paper explores the temporal and spatial

correlation of 3D ultrasonic signals for improved compression performance. The implementation of DWT based compression is optimised by determining the most suitable wavelet kernel and fine-tuning the decomposition structure based on frequency localisation. Furthermore, an efficient interpolation of decimated signals based on shift properties of Fourier transform is designed to precisely detect certain desirable features such as time-of-arrival and amplitude of ultrasonic echoes. Ultrasonic 3D RF data compression algorithms are analysed based on the degree of compression of RF data as a function of data integrity. The 3D implementation offers a CR of 95% with a PSNR of 27 dB for ultrasonic RF signals, supporting high quality signal reconstruction. The 3D compression using decimation is also found to be efficient for experimentation and data collection by eliminating unnecessary oversampling in spatial directions. DWT based compression is found to be efficient for hardware implementation because of its low resource usage. However, parallel execution of decimation/time-shift interpolation makes this compression method computationally more efficient.

7 References

1 Scabia, M., Biagi, E., Masotti, L.: 'Hardware and software platform for real-time processing and visualization of Echographic radio frequency signals', *IEEE Trans. Ultrason. Ferroelectr. Freq. Control*, 2002, **49**, (10), pp. 1444–1452

2 Saniie, J., Wang, T., Jin, X.: 'Performance evaluation of frequency diverse bayesian ultrasonic flaw detection', *J. Acoust. Soc. Am.*, 1992, **91**, (4), Pt. 1, pp. 2034–2041

3 Wang, T., Saniie, J., Jin, X.: 'Analysis of low-order autoregressive models for ultrasonic grain signal characterization', *IEEE Trans. Ultrason. Ferroelectr. Freq. Control*, 1991, **38**, (2), pp. 116–124

4 Daubechies, I.: 'Ten Lectures on Wavelets'. CBMS-NSF Regional Conference Series in Applied Math, SIAM, Philadelphia, 1992, vol. 61

5 Vetterli, M., Herley, C.: 'Wavelets and filter banks: theory and design', *IEEE Trans. Signal Process.*, 1992, **40**, (9), pp. 2207–2232

6 Ahmed, N., Natarajan, T., Rao, K.R.: 'Discrete cosine transform', *IEEE Trans. Comput.*, 1974, **C-23**, (1), pp. 90–93

7 Ahmed, N., Rao, K.R., Abdussattar, A.L.: 'BIFORE or Hadamard transform', *IEEE Trans. Audio Electroacoust.*, 1971, **19**, (3), pp. 225–234

8 Cheng, P.W., Shen, C.C., Li, P.C.: 'MPEG compression of ultrasound RF channel data for a real-time software-based imaging system', *IEEE Trans. Ultrason. Ferroelectr. Freq. Control*, 2012, **59**, (7), pp. 1413–1420

9 Cardoso, G., Saniie, J.: 'Performance evaluation of DWT, DCT and WHT for compression of ultrasonic signals'. IEEE Int. Ultrasonics, Ferroelectrics, and Frequency Control Joint 50th Anniversary Conf., 2004, vol. 3, pp. 2314–2317

10 Oruklu, E., Jayakumar, N., Saniie, J.: 'Ultrasonic signal compression using wavelet packet decomposition and adaptive Thresholding'. IEEE Ultrasonics Symp., 2008, pp. 171–175

11 Shi, G., Chen, C., Lin, J., Xie, X., Chen, X.: 'Narrowband ultrasonic detection with high range resolution: separating echoes via compressed sensing and singular value decomposition', *IEEE Trans. Ultrason. Ferroelectr. Freq. Control*, 2012, **59**, (10), pp. 2237–2253

12 Stanhill, D., Zeevi, Y.Y.: 'Two dimensional orthogonal wavelets with vanishing moments', *IEEE Trans. Signal Process.*, 1996, **44**, (10), pp. 2579–2590

13 Daubechies, I.: 'Orthonormal bases of compactly supported wavelets', *Commun. Pure Appl. Math.*, 1998, **XLI**, pp. 909–996

14 Keinert, F.: 'Wavelets and multiwavelets' (Chapman & Hall CRC, 2004)

15 Demirli, R., Saniie, J.: 'Model-based estimation of ultrasonic echoes part I: analysis and algorithms', *IEEE Trans. Ultrason. Ferroelectr. Freq. Control*, 2001, **48**, (3), pp. 787–802

16 Schafer, R.W., Rabiner, L.: 'A digital signal processing approach to interpolation', *IEEE Proc.*, 1973, **61**, (6), pp. 692–702

17 Brigham, E.: 'Fast Fourier transform and its applications' (Prentice Hall, 1974)

18 Proakis, J.G., Manolakis, D.G.: 'Digital signal processing: principles, algorithms and applications' (Pearson, 2011, 4th edn.)

19 Schwarz, K.: 'Linear phase FIR-filter in lattice structure', *IEEE Int. Symp. Circuits Syst.*, 1993, **1**, pp. 347–350

20 Desmouliers, C., Oruklu, E., Saniie, J.: 'Adaptive 3D ultrasonic data compression using distributed processing engines'. IEEE Int. Ultrasonics Symp., 2009, pp. 694–697

doi: 10.1049/iet-spr.2014.0186